

A Study on a Heavy Rainfall Event Triggered by an Inverted Typhoon Trough in Shandong Province*

ZHAO Yu^{1†}(赵 宇), CUI Xiaopeng²(崔晓鹏), and WANG Jianguo³(王建国)

¹ Nanjing University of Information Science & Technology, Nanjing 210044

² Laboratory of Cloud-Precipitation Physics and Severe Storms, Institute of Atmospheric Physics, Chinese Academy of Sciences, Beijing 100029

³ Henan Provincial Meteorological Bureau, Zhengzhou, Henan 450003

(Received November 26, 2008)

ABSTRACT

A heavy rainfall event that occurred in Shandong Province in 26–28 August 2004 was caused mainly by Typhoon Aere and cold air activities related to a westerly trough. The event was triggered by an inverted typhoon trough, which was closely associated with the intensification of the low-level southeasterly flow and the northward transport of heat and momentum in the periphery of the typhoon low. A numerical simulation of this event is performed using the nonhydrostatic mesoscale model MM5 with two-way interactive and triply-nested grids, and the structure of the inverted typhoon trough is studied. Furthermore, the formation and development mechanism of the inverted typhoon trough and a mesoscale vortex are discussed through a vorticity budget analysis. The results show that the heavy rainfall was induced by the strong convergence between the strong and weak winds within the inverted typhoon trough. Dynamic effects of the low-level jet and the diabatic heating of precipitation played an important role in the development of the inverted typhoon trough and the formation of the mesoscale vortex.

The vorticity budget analysis suggests that the divergence term in the low troposphere, the horizontal advection term, and the convection term in the middle troposphere were main contributors to positive vorticity. Nonetheless, at the same pressure level, the effect of the divergence term and that of the advection term were opposite to each other. In the middle troposphere, the vertical transport term made a positive contribution while the tilting term made a negative contribution, and the total vorticity tendency was the net result of their counteractions. It is found that the change tendency of the relative vorticity was not uniform horizontally. A strong positive vorticity tendency occurred in the southeast of the mesoscale vortex, which is why the heavy rainfall was concentrated there. The increase of positive vorticity in the low (upper) troposphere was caused by horizontal convergence (upward transport of vorticity from the lower troposphere). Therefore, the development of the inverted typhoon trough and the formation of the mesoscale vortex were mainly attributed to the vorticity generated in the low troposphere, and also the vertical transport of vorticity from the low and middle troposphere.

Key words: heavy rainfall event, landing typhoon, inverted typhoon trough, vorticity budget

Citation: Zhao Yu, Cui Xiaopeng, and Wang Jianguo, 2009: A study on a heavy rainfall event triggered by an inverted typhoon trough in Shandong Province. *Acta Meteor. Sinica*, **23**(4), 468–484.

1. Introduction

Typhoon Aere was generated in the northwestern Pacific Ocean in the morning of 20 August 2004, and made a landfall in Fuqing County of Fujian Province at 1630 BT (Beijing Time) 25 August, with a maximum central wind speed of 35 m s^{-1} . Then, it moved into Guangdong Province along the southeastern coastline

of Fujian Province. In the afternoon of 26 August, it weakened into a tropical depression and stagnated in Guangdong Province. An extremely heavy rainfall event occurred in Shandong Province in 26–28 August 2004. The event was influenced by the typhoon depression and a westerly trough. Torrential rain occurred in most parts of Shandong Province, with the 3-h rainfall amount exceeding 50 mm at some stations.

*Supported by Wuhan Institute of Heavy Rain, China Meteorological Administration, under Grant No. IHR2008K03, and the Scientific Research Project of the Shandong Provincial Meteorological Bureau under Grant No. 2006sdqxz18.

[†]Corresponding author: zy0817@126.com.

For example, the rainfall amount at Chengwu County reached 80.9 mm from 1400 to 1700 BT 27 August, resulting in serious flooding and bad traffic in parts of the city.

The heavy rainfall was caused by the interaction between the mid- and low-latitude systems and it belongs to a type of rainstorms occurring far away from a typhoon. Due to the importance and complexity of the interaction between the mid- and low-latitude systems, researchers at home and abroad have paid much attention to this type of rainstorms, and a lot of important findings have been achieved. Palmén (1958) and Anthes (1990) examined the large-scale dynamics associated with the extratropical transition (ET) of Hurricane Hazel moving into the United States. Their studies indicated that the transport of tropical air mass into the midlatitudes resulted in a large increase in the available potential energy (APE) of the atmosphere, and the approaching midlatitude trough provided a mechanism by which this APE was converted to kinetic energy through thermally direct circulations, resulting eventually in a rather powerful extratropical cyclone. Many researchers discussed the dynamic mechanism and strong precipitation caused by the interaction between Hurricane Agnes and the midlatitude trough. Bosart and Carr (1978) examined the precipitation case several hundred kilometers ahead of Agnes and pointed out that the heavy rains were located in a confluent flow region between a weak midlatitude trough and the outflow ridge associated with Agnes. DiMego and Bosart (1982a, b) found that Agnes re-intensified and then underwent the ET as the large-scale ascent ahead of the approaching trough overspread the periphery of the remnant low-level circulation. Atallah and Bosart (2003) discussed the ET of Hurricane Floyd and its precipitation distribution from the viewpoint of potential vorticity, and obtained instructional results.

In the 1970s, Chinese meteorological researchers systematically studied the formation of the “75.8” torrential rain that occurred in Henan Province. The “96.8” torrential rain, which caused a great loss in Hebei and Shanxi provinces, has been the heaviest since the “63.8” heavy rain in Hebei Province. Jiang

and Xiang (1997) studied its formation by using routine observational data and satellite images. In addition, Feng et al. (2000) and Sun et al. (2006) thoroughly studied meso- β systems producing the heavy rainfall by employing numerical simulations. In recent years, with the continuous development and perfection of mesoscale models, numerical simulations have been widely used to study heavy rainfalls (e.g., Bei et al., 2003; Sheng et al., 2006; Yang et al., 2007; Yang and Gao, 2007) and the interaction between mid- and low-latitude systems (e.g., Zhu et al., 2002a,b; Li et al., 2005; Ye et al., 2007).

In a sense, it is the inverted typhoon trough rather than the typhoon depression itself that may have a more direct impact on the weather in eastern Asia (Sun and Zhao, 2000). Due to water vapor transport from the typhoon, the rainfall ahead of midlatitude westerly troughs and far away from a typhoon usually becomes significant (Zhu et al., 2000). Therefore, it is crucial to take into account the far-distance effect of a typhoon in forecasting such heavy rainfall events. Jiang et al. (1981) and Jiang (1983) proposed a conceptual model for the type of rainstorms affected by a far-distance typhoon, and systematically studied the related mechanisms. Ding and Chen (1995) and Ding et al. (2001) investigated the positive feedback between the non-zonal high-level jet streak and the far-distance typhoon-induced rainstorm by using statistical methods and numerical simulations. The above studies disclosed the reasons for the formation of rainstorms far away from a typhoon from different angles.

Heavy rainfall events are largely caused by meso- and micro-scale systems. However, meso- and micro-scale observational data are scarce, which has restricted the studies on this topic. At present, systematic studies on mesoscale dynamics of rainstorms affected by a far distance typhoon are not enough. In particular, the formation and development processes of inverted typhoon troughs triggering rainstorms and associated mesoscale systems remain unclear. Because mesoscale models are able to provide high-resolution (in both space and time), dynamically consistent data, they can be used as a powerful tool to study mesoscale

weather systems. In this paper a rainstorm that occurred far away from a typhoon is studied using the mesoscale model MM5. The structural characteristics of an inverted typhoon trough and a mesoscale vortex as well as their genesis and development mechanisms are given, and the relationship between the mesoscale convective systems within the inverted typhoon trough and the typhoon circulation is discussed. Furthermore, the interaction among the evolution of dynamic and thermodynamic fields, the typhoon circulation and mesoscale convective systems is revealed. The purpose of the present study is to provide some guidance for the forecast of rainstorms being affected by a far-away typhoon.

2. Rainfall observation and the inverted typhoon trough

Distributions of the observed 3-h rainfall show that precipitation started at 1600 BT 26 August, and a small rainy area first emerged in southwestern Shandong Province and then extended northeastward. The rain continued to stay in southwestern Shandong and the central Shandong hilly area from 2000 BT 26 to 2000 BT 27 August. This is defined as the first phase (period) in this study. Afterwards, the rainy area moved eastward. The rainfall event in Shandong persisted until noon 28 August. The period from 2000 BT 27 to 1200 BT 28 August is defined as the second phase (period). Figure 1a shows the observed accumulated rainfall from 0800 BT 26 to 0800 BT 28 August. The precipitation center was in the southwestern part of

Shandong Province, with a maximal rainfall of 210.4 mm in Jinxiang County (35.1°N, 116.3°E). Rain gauge observations at about 20 counties (cities) exceeded 100 mm and the average rainfall over Shandong Province was 62.5 mm.

The heavy rainfall occurred under a special large-scale environment. The NCEP FNL global analysis data reveals that by 2000 BT 26 August 2004, at 200 hPa, a very strong upper level jet was located to the north of 38°N (Fig.2a). At 500 hPa, a deep cold vortex was located in Lake Baikal. A westerly trough passing through the center of the cold vortex extended southward to around 40°N, and another short-wave trough was located in the Hetao area (Fig.2a). The cold vortex continuously split cold air and traveled southward, keeping the Hetao area under the influence of the westerly trough for a long time, while southwesterly currents dominated Shandong Province. The subtropical high was weak and shifted to the east. At 700 hPa, a branch of the southeasterly jet formed in the northeastern side in the periphery of the typhoon depression, crossed the Huaihe River Basin, and traveled into the southwestern part of Shandong Province from 0800 BT 26 August (figure omitted). At 850 hPa, the inverted typhoon trough began to extend to the southwestern part of Shandong Province at about 2000 BT 26 August and intensified obviously and stretched northward at 0800 BT 27 August (Fig. 2b). The inverted typhoon trough joined the westerly trough at 2000 BT 27 August. At the surface level, the inverted trough started to extend to the southwestern part of Shandong Province at about 1400 BT 26 August

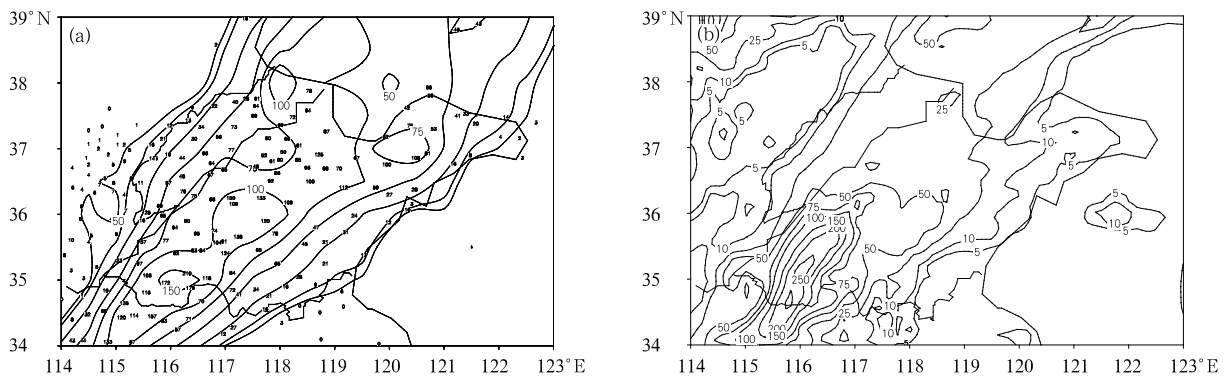


Fig. 1. Observed (a) and simulated (b) rainfall (mm) from 0800 BT 26 to 0800 BT 28 August 2004. Isopleths are 5, 10, 25, 50, 75, 100, 150, 200, and 250 mm.

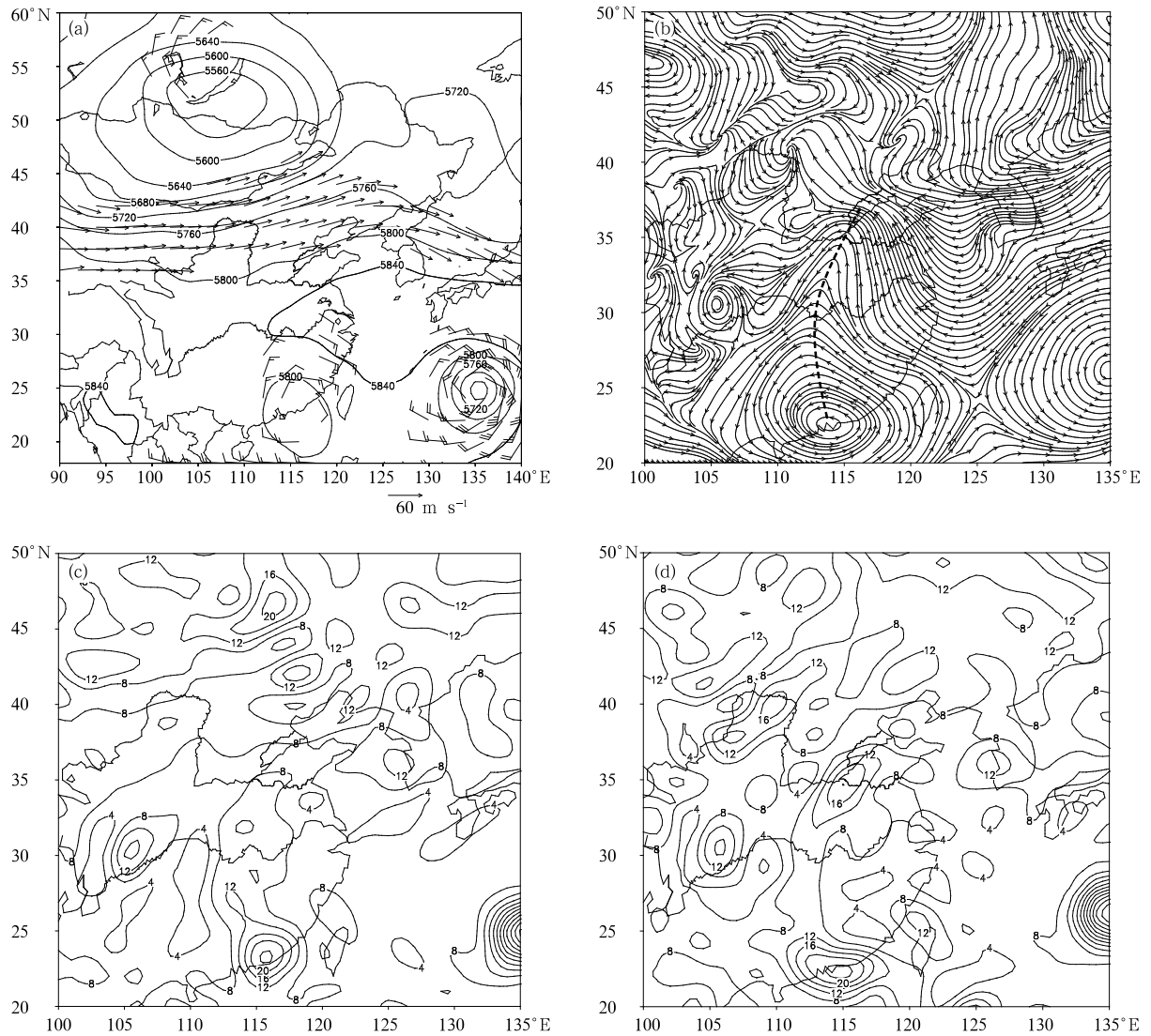


Fig. 2. (a) Comprehensive synoptic pattern distributions at 2000 BT 26 August 2004 (solid lines represent 500-hPa geopotential height in gpm, arrows are 200-hPa wind vectors with speed $\geq 40 \text{ m s}^{-1}$, and barbs represent 850-hPa wind vectors with speed $\geq 12 \text{ m s}^{-1}$). (b) The 850-hPa streamline field at 0800 BT 27 August 2004 (the thick dashed line denotes the inverted typhoon trough). (c) and (d) are 850-hPa vorticity distributions at 2000 BT 26 and 0800 BT 27 August 2004, respectively. The results in this figure are derived from the NCEP FNL global analysis data.

(figure omitted). The heavy rainfall was first triggered to the north of the inverted typhoon trough. The southern Shandong and the southern part of the central Shandong hilly area were located to the north of the inverted typhoon trough, in the left of the low-level jet and the right of the upper level jet, which constitutes a favorable environment for the formation of the heavy rainfall. The precipitation in the first period was produced by the inverted typhoon trough, and in the second period it was attributed to the inter-

action between the inverted typhoon trough and the westerly trough.

3. Experimental design and verification of model results

3.1 Experimental design

The PSU-NCAR mesoscale model MM5 is chosen to simulate the heavy rainfall event. Triply-nested domains are used (Fig. 3). The three domains D01,

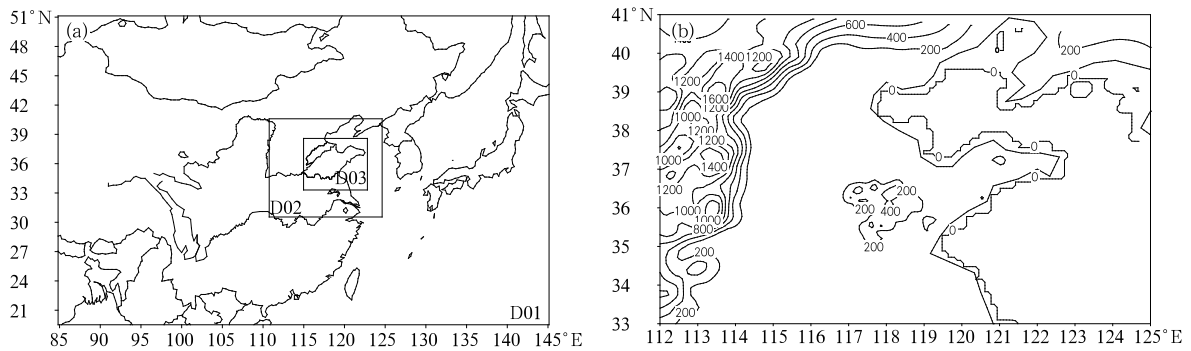


Fig. 3. Triply nested grid domains (a) and terrain height in D02 (b).

D02, and D03 have 82×61 , 67×55 , and 136×100 horizontal grid points, with resolutions of 54, 18, and 6 km, respectively. In the vertical, the model consists of 23 sigma levels, with the model top at 100 hPa.

The physical parameterizations used in the simulation include the Kain-Fritsch cumulus scheme, Reisner graupel explicit-moisture scheme, time-dependent lateral boundary condition, MRF planetary boundary layer scheme, cloud-radiation scheme, and a five-layer soil model. The shallow cumulus scheme is switched on at all nested grids. The NCEP FNL global analysis data with a 1° horizontal resolution and 6-h intervals are used as initial fields, and the conventional surface and upper air sounding observations at 12-h intervals are incorporated into the initial and lateral boundary conditions using an objective analysis. The simulation starts from 0800 BT 26 August and ends at 2000 BT 28 August 2004.

3.2 Simulation results

Figure 1b illustrates the simulated 48-h accumulated rainfall. It can be seen that the simulated rainfall coverage and amount match very well with the observation (Fig. 1a). The location and order of magnitudes of the simulated rainfall center are close to those of the observation except that the area with rainfall ≥ 200 mm is a bit larger and the rainfall in northern Shandong is smaller than the observed.

A comparison of 6-h accumulated rainfall between the simulation and the corresponding observation shows that a small rainy area located in the southwestern part of Shandong Province was first reproduced by the model in the evening of 26 August,

with the rainfall coverage and amount being smaller than those observed from 1400 to 2000 BT 26 August (Fig. 4a). There were some differences between the simulated and observed rainfall locations from 2000 BT 26 to 0200 BT 27 August (Fig. 4b). Although the model did produce rainfall in southern Shandong, the rainfall center was shifted to the west compared with the observation, and the rainfall in the middle and northern part of Shandong Province was not well captured. This probably results from the spin-up time of the model. After the model was integrated for 18 h at 0200 BT 27 August, the simulation corresponded very well with the observation, and just around this time, the mesoscale systems developed and came into play. This is the time we choose for detailed analysis in this study. Notably, the simulation agreed well with the observation in both the rainfall coverage and amount from 0200 BT to 2000 BT 27 August (Figs. 4c-e). The simulated rainfall center (75 mm) was quite close to the observation (77 mm) except that the former was shifted to the east of the latter from 0800 to 1400 BT 27 August (Fig. 4d).

In the next 6 h, the simulated rainfall center was shifted to the north about 50 km from the observation, and the central rainfall amount reached about 100 mm while the observed maximum rainfall at Jinxiang County was 99.1 mm from 1400 to 2000 BT 27 August (Fig. 4e). Although the model successfully captured the movement of the rainy area to the eastern part of the central Shandong hilly area and the intensification of the northern rainy area during the second period, it produced false rainfall in the southwestern part of Shandong Province from 2000 BT 27 to 0200 BT 28

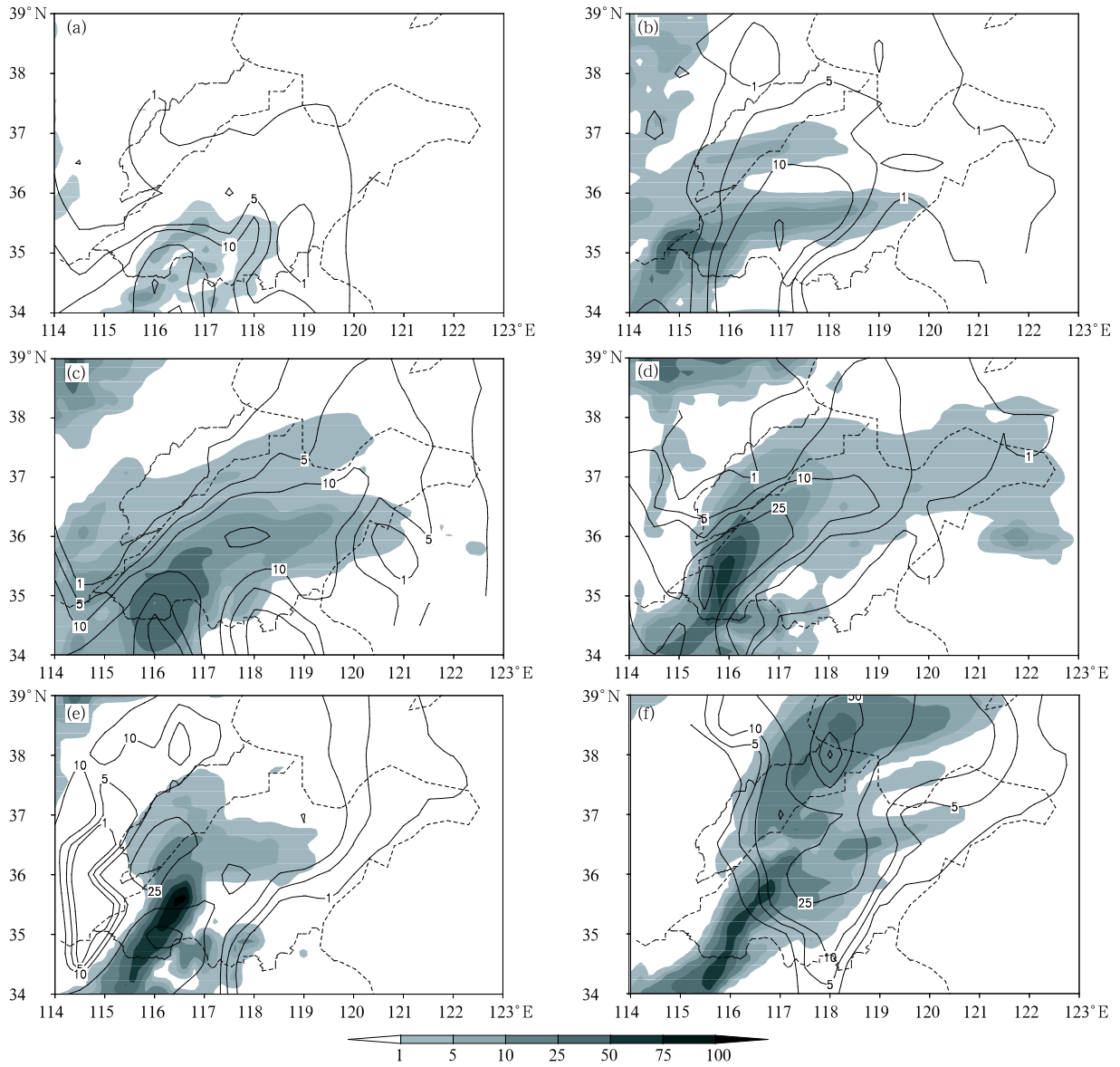


Fig. 4. Observed (contours: 1, 5, 10, 25, 50, 75, 100) and simulated (shadings) 6-h rainfall (mm) at (a) 1400–2000 BT 26 August, (b) 2000 BT 26 to 0200 BT 27 August, (c) 0200–0800 BT 27 August, (d) 0800–1400 BT 27 August, (e) 1400–2000 BT 27 August, and (f) 2000 BT 27 to 0200 BT 28 August.

August (Fig. 4f). Moreover, the simulated rainfall amount in the northern part of Shandong Province was less than that observed, and the simulated eastward movement of the rainy area was slower from 1400 to 2000 BT 27 August (figure omitted). Furthermore, precipitation in western Shandong had actually ended whereas there was still rainfall in this area in the simulation. In summary, the model generally reproduced the occurrence and duration of the heaviest rainfall with the simulated rainfall location and intensification

being consistent with the observation. The genesis, development, and evolution of the mesoscale rainstorm systems during the first period (2000 BT 26 to 2000 BT 27 August) are the focus of this study, so the simulation deficiencies prior to and after this period shall not harm the results of the analysis.

Comparisons of the synoptic patterns show that the typhoon depression, the cold vortex located in Lake Baikal, the westerly trough, the inverted typhoon trough, etc. and their evolution were all reproduced

successfully. In short, the model did reasonably reproduce the formation and development of the heavy rainfall event.

4. The inverted typhoon trough

Distributions of the absolute vorticity calculated by using the NCEP FNL global analysis data at 6-h intervals illustrate that the typhoon depression was associated with a positive vorticity center. During the intensification of the low-level southeasterly jet, positive vorticity was transported northward from the positive vorticity area of the typhoon depression at 850 and 925 hPa, resulting in obvious development of positive vorticity in the southwestern part of Shandong Province. At 850 hPa, the high value area of positive vorticity was located south of Shandong Province, and a positive vorticity belt ($> 8 \times 10^{-5} \text{ s}^{-1}$) in connection with the typhoon depression extended northward into the southwestern part of Shandong Province at 2000 BT 26 August (Fig. 2c). The positive vorticity in southwestern Shandong started to enhance from 0200 BT 27 August. At 0800 BT 27 August (Fig. 2d), a new belt with positive vorticity larger than $8 \times 10^{-5} \text{ s}^{-1}$ formed there and the central value was $20 \times 10^{-5} \text{ s}^{-1}$, which corresponded with the significant development of the inverted typhoon trough (Fig. 2b). Obviously, the development of the inverted typhoon trough was associated with the intensification of the low-level southeasterly jet and the northward transport of momentum in the periphery of the typhoon depression. Distributions of the temperature advection (figure omitted) indicate that the development of the inverted typhoon trough was accompanied by warm advection. So the questions to be addressed are: what was the mesoscale structure of the inverted typhoon trough? How did it develop and interact with the typhoon depression?

4.1 Low-level streamline fields

To further reveal the mesoscale structure of the inverted typhoon trough and the role of its development and evolution in the heavy rainfall event, the MM5 simulated low-level streamline and hourly rainfall fields are analyzed. Around 2000 BT 26 August,

the inverted typhoon trough firstly extended to the southwestern part of Shandong Province at 925 hPa. Three hours later, at 2300 BT 26 August, the inverted typhoon trough developed vertically into 850 hPa, while at 925 hPa it developed further northward, with rainfall occurring at upper levels and tilting to the warm and moist southeasterly flow side. The rainfall intensity was larger from 0000 BT to 0200 BT 27 August, reaching 20–30 mm h^{-1} (Fig. 5a), and afterwards, the inverted typhoon trough weakened. By 0500 BT 27 August (Fig. 5b), with the intensification of the warm and moist southeasterly flow, the inverted typhoon trough re-intensified to the east of the old one, extended northward noticeably, and gradually traveled northwestward. At 1000 BT 27 August, the curvature of the inverted typhoon trough started to increase markedly (Fig. 5c) and a mesoscale vortex formed in the northern part of the inverted trough at 1400 BT 27 August. At 1600 BT 27 August, the mesoscale vortex became very intensive and the 1-h accumulated rainfall reached 30–50 mm, with rainfall occurring in the east of the vortex. After sustaining for 4 h at the same place, the mesoscale vortex weakened and disappeared. The formation of the mesoscale vortex corresponded with the occurrence of the heaviest rainfall, and the model simulated rainfall intensity during this period was 20–30 mm h^{-1} .

The streamline distribution at 850 hPa was similar to that at 925 hPa (figure omitted). The cyclonic circulation on top of the inverted trough started to intensify at 1100 BT 27 August and a mesoscale vortex formed at 1500 BT 27 August. The mesoscale vortex weakened and disappeared after sustaining for 3 h. It is obvious that the inverted typhoon trough and the mesoscale vortex developed upward from lower levels. There was no appearance of the inverted typhoon trough and the mesoscale vortex at and above 700 hPa. Southerly winds dominated at 700 hPa, and a weak cyclonic curvature appeared, corresponding to the lower-level mesoscale vortex. After 2100 BT 27 August, rainfall occurred again because of the interaction between the inverted typhoon trough and the westerly trough, but the rainfall intensity was remarkably weak, with the maximal rainfall intensity

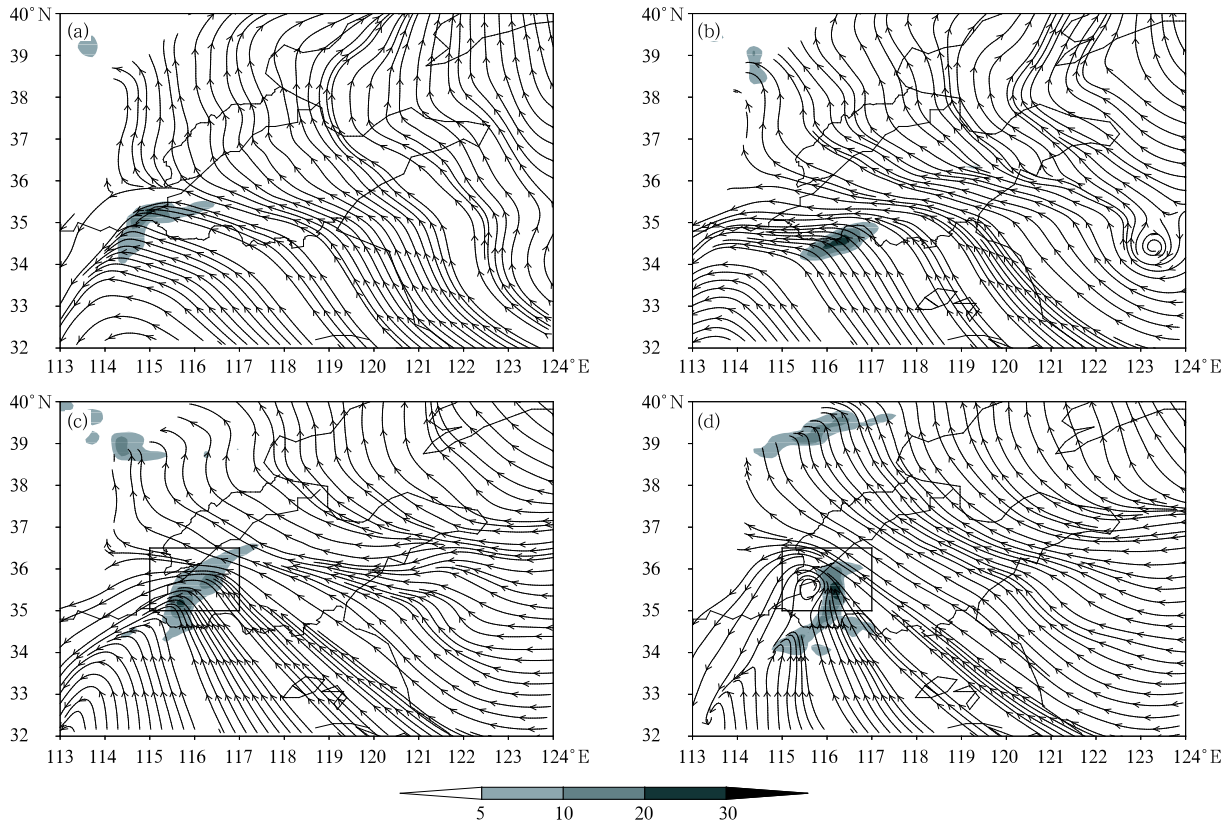


Fig. 5. Simulated 925-hPa streamline fields and 1-h accumulated rainfall (shadings; mm) at (a) 0200 BT, (b) 0500 BT, (c) 1000 BT, and (d) 1400 BT 27 August. The rectangles in (c) and (d) denote domain A.

of $10\text{--}20\text{ mm h}^{-1}$. The northeast to southwest oriented zonal rain belt was located in the southeasterly wind ahead of the junction between the northerly and southeasterly winds.

4.2 Low-level wind, vorticity and divergence fields

Figure 6 shows that at 925 hPa, following the intensification of the warm and moist southeasterly flow, strong winds south of Shandong Province got intensified gradually and marched northwestward. Accompanying the intensification of the inverted typhoon trough, weak winds in southern Hebei and Henan provinces traveled to southwestern Shandong. By 0100 BT 27 August (Fig. 6a), strong winds of 12 m s^{-1} formed in southern Shandong, and weak winds below 2 m s^{-1} formed in the north of Henan Province. Thus, a large wind gradient appeared in southwestern Shandong. The heavy rainfall just occurred in the large wind gradient zone above the inverted ty-

phoon trough, where the cyclonic warm shear was the strongest. It can be seen from vertical cross-sections (figure omitted) that $\frac{\partial\theta_e}{\partial p}$ was greater than zero below 700 hPa nearby the inverted typhoon trough, showing convective instability over there. Notably, southeasterly winds south of the inverted typhoon trough brought abundant warm and moist air and instable energy from the sea and created convective instability in the lower troposphere. The large wind gradient zone formed between the strong and weak wind areas ahead of the inverted typhoon trough, resulted in low-level convergence, triggered the upward motion, and easily produced intense convective weather and thunderstorm activities. The distributions of divergence and vorticity exhibit that the inverted typhoon trough was located in an obvious convergent area (Fig. 6c) with negative vorticity at 850 hPa and positive vorticity at 500 hPa (figure omitted).

It is found that such a structure of upper-level positive vorticity and low-level convergence

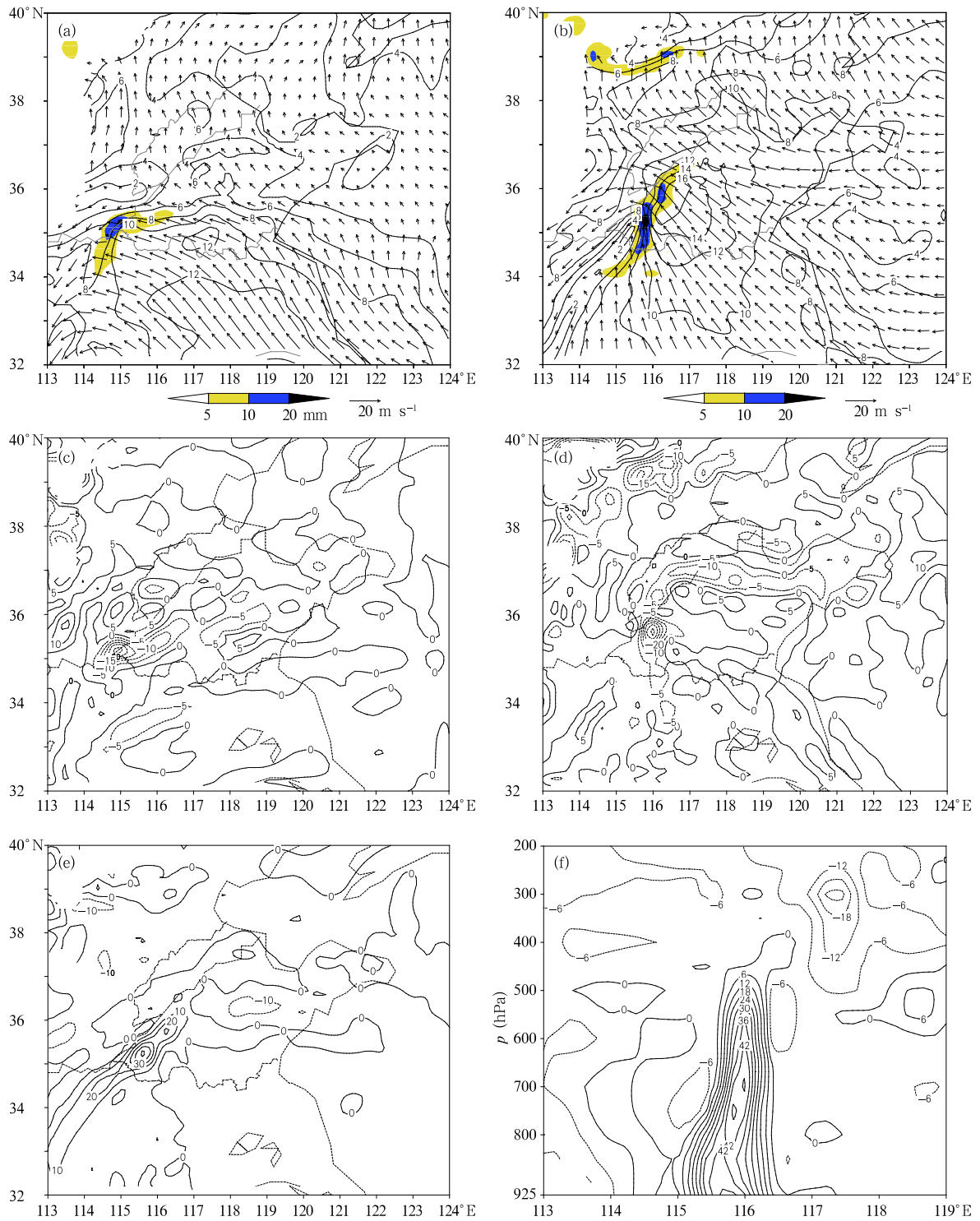


Fig. 6. Simulated 925-hPa wind vectors and isotaches (a, b; m s^{-1}), 850-hPa divergence (c, d; 10^{-5} s^{-1}), 850-hPa vorticity (e; 10^{-5} s^{-1}), and the latitudinal-height cross-section of vorticity (10^{-5} s^{-1}) along 35.5°N (f) at 0100 BT (a, c), 1100 BT (b), 1300 BT (d, f), 1000 BT (e) 27 August. Shadings denote 1-h rainfall (mm).

in southwestern Shandong occurred from 2200 BT 26 August, simultaneously with the heavy rainfall. Apparently, no positive vorticity was transported northward during the first development period (2000 BT 26 to 0200 BT 27 August; see the first paragraph in Section 4.1) of the inverted typhoon trough, so it was weak in this period of time.

Accompanying the second development of the inverted typhoon trough from 0500 to 1400 BT 27 August, the strong wind center in the south re-intensified and moved northward into Shandong Province. At 0600 BT 27 August, a wind speed core of 14 m s^{-1} formed in Zhou County, and to its southwest, a weak wind zone in Henan Province gradually penetrated northeastward. At 1100 BT 27 August (Fig. 6b), a strong wind speed center of 16 m s^{-1} advanced to the south of the central Shandong hilly area, while a weak wind speed center of 2 m s^{-1} entered into southwestern Shandong, and another weak wind speed center was in central Hebei Province. Therefore, a strong wind gradient zone formed between the strong and weak wind areas, and heavy rainfall occurred right within the large wind gradient area. At 1400 BT 27 August, a mesoscale vortex was generated in the weak wind zone in southwestern Shandong. The outboard winds in the north, east and west of the mesoscale vortex were greater than those inboard, which resulted in cyclonic shears favorable for the production of positive vorticity.

Jiang et al. (2003) and Zhao et al. (2006) indicated that strong rainfall mainly occurred at large wind gradient zones between mid- and low-level “wind speed mates” (strong and weak wind centers), and the “wind speed mate” was probably a triggering mechanism for the heavy rain. These were confirmed again in this study. Distributions of vorticity and divergence at 850 hPa show that a northeast to southwest oriented convergence belt with positive vorticity in northern Anhui Province began to move to southwestern Shandong from 0500 BT 27 August, and it was intensified saliently when it entered into Shandong Province. By 1000 BT 27 August, a narrow positive vorticity belt was located in southwestern Shandong with a central value of $55 \times 10^{-5} \text{ s}^{-1}$, and it maintained with such

a strength until the mesoscale vortex was generated (Fig. 6e). At 1300 BT 27 August, the convergence center (Fig. 6d) with positive vorticity (figure omitted) above the inverted typhoon trough became extremely strong: the convergence and positive vorticity values were $-30 \times 10^{-5} \text{ s}^{-1}$ and $60 \times 10^{-5} \text{ s}^{-1}$, respectively, which created advantageous conditions for the formation of the mesoscale vortex. After the formation of the mesoscale vortex, the positive vorticity center weakened a little but still maintained at a central value of $40 \times 10^{-5} \text{ s}^{-1}$. The change of vorticity at 500 hPa was similar to that at 850 hPa except that the intensification was less intensive. It is obvious that the positive vorticity in the lower troposphere played a more important role in the development of the inverted typhoon trough and the formation of the mesoscale vortex than that in the upper troposphere.

It can be seen from cross-sections of vorticity and divergence fields along 35.5°N that positive vorticity over the rainy area started to strengthen markedly at 1100 BT 27 August due to the overlapping and coupling of positive vorticity centers in the upper and lower troposphere (figure omitted). A strong positive vorticity column was found below 450 hPa, and a negative vorticity column was above that. One hour later, the low-level positive vorticity column developed intensely with its central value reaching $54 \times 10^{-5} \text{ s}^{-1}$, which was conducive to the generation of the mesoscale vortex. At 1300 BT 27 August (Fig. 6f), below 800 hPa, the positive vorticity split and another positive vorticity center formed in the surface layer, suggesting that a meso- β rainstorm system was brewing in response to the mesoscale vortex in the lower troposphere. Afterwards, the positive vorticity column extended further upward, indicating that the system was intensifying. By 1600 BT 27 August, the positive vorticity column extended into 300 hPa and slanted to the east above 500 hPa, showing that vorticity was weak above 500 hPa, which was favorable for the formation of the heavy rainfall event.

It is doubtless that the intensification of the inverted typhoon trough and the formation of the mesoscale vortex were closely associated with the low-level jet and its dynamic effects. Due to the

intensification of the southerly current in the peripheries of the subtropical high and the typhoon, southerly momentum was carried continuously northward. Due to the blockage of the inverted typhoon trough, the momentum was congregated in southwestern Shandong and high wind speed cores (low-level jet) formed at 925 and 850 hPa. To the left of the low-level jet was cyclonic shear, which produced cyclonic vorticity in favor of the development of the low-level vortex. At the same time, the convergent wind area moved northward into southwestern Shandong under the compelling low-level southeasterly current. The evident increase of low-level convergence led to the intensification of positive vorticity, and then the development of the inverted typhoon trough. In addition, the southwestern Shandong area is situated at the right side of the entrance of the upper level jet (Fig. 2a), where a secondary circulation with upward motion might form between the upper- and low-level jets. The intensification of low-level convergence and positive vorticity as well as the effect of latent heat release produced by rainfall resulted in the formation of the mesoscale vortex. The strong convergence effect of the mesoscale vortex promoted the intensive development of the upward motion, and the upper-level divergence was further enhanced, which strengthened the vertical pumping of the mesoscale systems. Due to the law of mass continuity, the low-level convergence would be further increased, and the upper- and low-level systems produced a positive feedback, leading to the heavy rainfall.

4.3 The development of the inverted typhoon trough and the mesoscale vortex

4.3.1 Vorticity budget analysis

The above analyses indicated that the occurrence and development of the inverted typhoon trough and the mesoscale vortex were associated with the transport of positive vorticity and the superposition or the coupling of positive vorticity centers in the upper and lower troposphere. This seems to imply that the horizontal and vertical transport of vorticity played an important role. Therefore, we now calculate contributions of the various terms of the vorticity equation to study the physical processes of vorticity generation

and development.

By neglecting the friction and the vertical transport effects of cumulus on vorticity, the vorticity equation in the pressure coordinate can be written as:

$$\frac{\partial \zeta}{\partial t} = -\left[\left(u \frac{\partial \zeta}{\partial x} + v \frac{\partial \zeta}{\partial y} + w \frac{\partial \zeta}{\partial p}\right) - (\zeta + f) \left(\frac{\partial u}{\partial x} + \frac{\partial v}{\partial y}\right) + \left(\frac{\partial w}{\partial y} \frac{\partial u}{\partial p} - \frac{\partial w}{\partial x} \frac{\partial v}{\partial p}\right)\right]. \quad (1)$$

Here, f is the Coriolis parameter, and ζ is relative vorticity. The term on the left is the local variation of relative vorticity (ζ_{ten}). The first term on the right is the horizontal advection term (ζ_{hadv}), which is caused by non-uniform horizontal distribution of relative vorticity. The second term on the right is the convection term (ζ_{vadv}), which represents local change of vorticity resulted from the redistribution of relative vorticity due to vertical motion in the non-uniform vorticity field. The third term on the right is the divergence term (ζ_{div}), denoting the amplification (reduction) of vertical vorticity caused by horizontal convergence (divergence). The fourth term on the right is the tilting term (ζ_{tilt}), representing the change of vertical vorticity due to non-uniform horizontal distributions of the vertical motion when there exists horizontal vorticity. The summation of all terms on the right side represents the magnitude of the local change of relative vorticity.

To investigate how the positive vorticity was produced within the inverted typhoon trough, various terms of the vorticity equation regionally averaged over domain A (35° – 36.5° N, 115° – 117° E; the panel in Figs. 5c and 5d, covering the area of the inverted typhoon trough and the mesoscale vortex) were calculated. We selected three time moments: 1000 BT 27 August when the inverted typhoon trough began to develop intensively, 1400 BT 27 August when the mesoscale vortex was generated, and 1800 BT 27 August when the mesoscale vortex disappeared, to study changes of the various terms of the vorticity equation.

It can be seen from Fig. 7 that the local change of vorticity at 850 hPa was appreciable in southwestern Shandong when the inverted typhoon trough began to develop intensively and the mesoscale vortex formed. Positive (negative) vorticity tendency appeared in

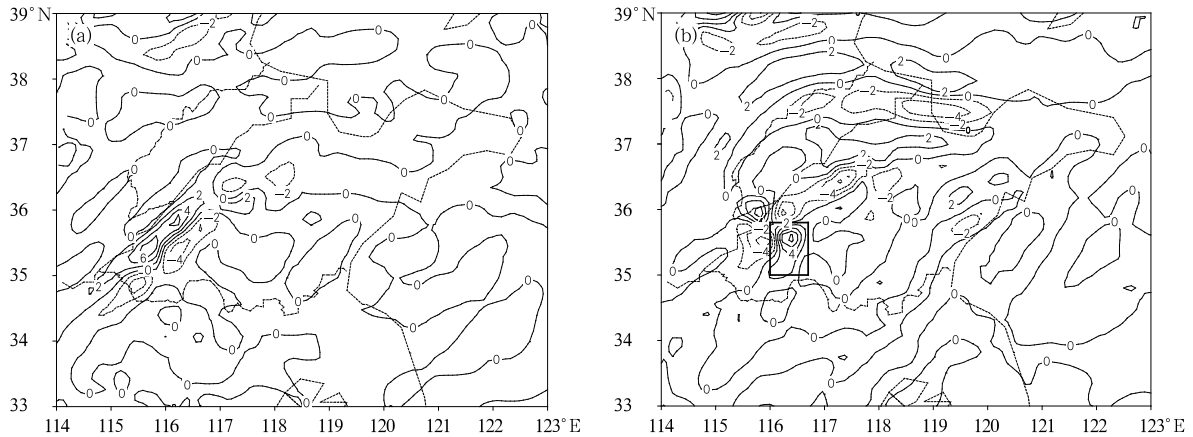


Fig. 7. Local tendency of vorticity (10^{-8} s^{-2}) at 850 hPa at 1000 BT (a) and 1400 BT (b) 27 August. The rectangle in (b) denotes domain B.

pairs and in a staggered manner in southwestern Shandong. At 1000 BT 27 August, two strong positive (negative) vorticity tendency centers were observed where the inverted typhoon trough was, with a maximal positive vorticity change of $6 \times 10^{-8} \text{ s}^{-2}$. By 1400 BT 27 August (Fig. 7b), two pairs of positive (negative) vorticity tendency centers were staggered, with the negative centers oriented northeast to southwest and the positive centers oriented from northwest to southeast. The mesoscale vortex was shallow and only existed in the lower troposphere between 850 and 925 hPa. The vorticity tendency at various levels over the inverted typhoon trough and the mesoscale vortex were not completely consistent, then, how were the vertical distributions of the various terms of the vorticity equation?

Figure 8a illustrates the vertical profiles of the various terms of the vorticity equation at 1000 BT 27 August. It can be seen that notable positive tendency existed below 400 hPa, among which the maximum reached $0.8 \times 10^{-8} \text{ s}^{-2}$ at around 925 hPa, and a secondary maximum was located at about 650 hPa. Positive vorticity tendency meant that cyclonic vorticity increased with time, which was consistent with the curvature increase and intensive development of the inverted typhoon trough. The divergence term produced by intense low-level convergence made a positive (negative) contribution to the vorticity tendency below (above) 720 hPa. The horizontal advection term

contributed positively (negatively) to the vorticity tendency below (above) 780 hPa. The tilting term made a negative contribution while the convection term made a positive contribution throughout the whole troposphere. Obviously, the effects of the horizontal advection term and the divergence term were opposite to each other at the same pressure level, so were the effects of the tilting term and the convection term. The contribution of the divergence term was greater than that of the horizontal advection term in the lower and middle troposphere. The contribution of the convection term was more than that of the tilting term in the middle troposphere. The net result of these counteractions was that strong vorticity tendency appeared in the boundary layer (around 925 hPa) and the middle troposphere, which was favorable for the intensification of the upward motion as well as the development of the inverted typhoon trough, and then the enhancement of rainfall. The pronounced development of the inverted typhoon trough was mainly produced by the intensification of convergence in the lower troposphere and the enhancement of vertical transport of vorticity.

At 1400 BT 27 August (Fig. 8b), the vorticity tendency throughout the troposphere was weaker than that at 1000 BT 27 August, with the maximal vorticity tendency of $0.3 \times 10^{-8} \text{ s}^{-2}$ at 500 hPa and weak negative vorticity tendency between 900 and 700 hPa. This was due to the change of the convection and the tilting terms. The negative tilting term and the

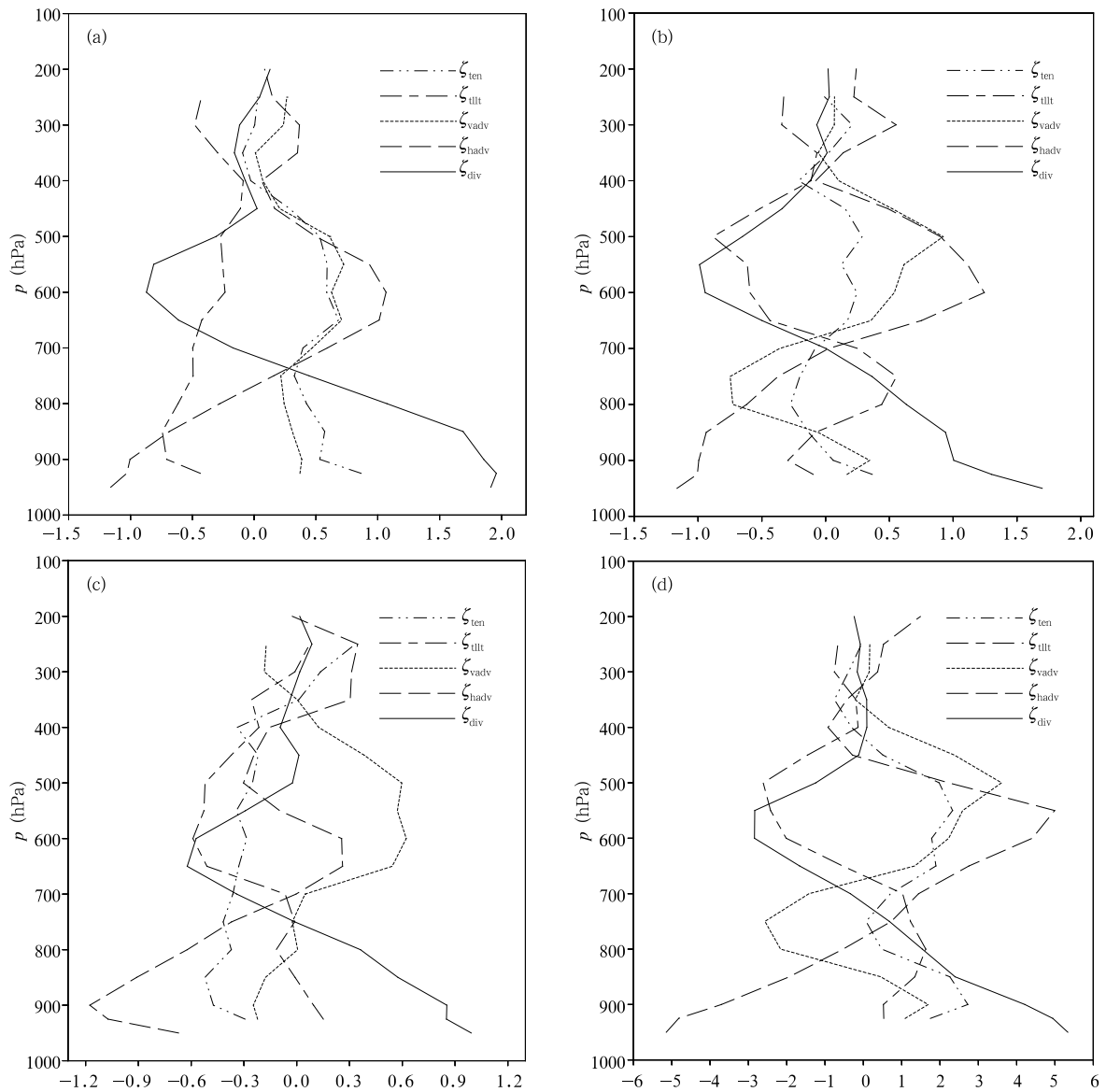


Fig. 8. Vertical profiles of the various regionally averaged terms (10^{-8} s^{-2}) of the vorticity equation at 1000 BT (a), 1400 BT (b), 1800 BT 27 August (c) over domain A (see Fig. 5d), and 1400 BT 27 August (d) over domain B (see Fig. 7b).

positive convection term compensated each other between 700 and 400 hPa. The tilting term was positive and the convection term was negative from 850 to 700 hPa. Although the effects of the divergence term and the horizontal advection term were opposite to each other in the upper and lower troposphere, the balanced result of all terms of the vorticity equation led to weak vorticity tendency throughout the troposphere. It can be seen from Fig. 7b that two couplets of positive (neg-

ative) vorticity tendency were staggered in domain A. Perhaps the co-existence of the positive (negative) couplet weakened the local change of vorticity over that area. Thus, we calculate the vorticity budget over the area where the local change of vorticity was positive.

Figure 8d illustrates the vertical profiles of the various terms of the vorticity equation averaged over domain B (35° – 35.8° N, 116° – 116.7° E; the rectangle in Fig. 7b), which covers the southeastern quadrant of

the mesoscale vortex, at 1400 BT 27 August 2004. It can be seen that: 1) positive vorticity tendency under 400 hPa was larger than that in Fig. 8b; 2) the maximal vorticity tendency reached $2.7 \times 10^{-8} \text{ s}^{-2}$ around 900 hPa; 3) the second maximum was $2.3 \times 10^{-8} \text{ s}^{-2}$ at about 550 hPa; 4) the vorticity tendency in the middle troposphere was also large. Below 800 hPa, besides the negative contribution made by the horizontal advection term, the other three terms made positive contributions. The positive divergence term counteracted with the negative horizontal advection term, and the positive vorticity tendency in the lower troposphere was mainly resulted from the effects of the convection term and the tilting term. Meanwhile, between 700 and 400 hPa, positive horizontal advection contribution was greater than negative divergence contribution, and the convection term was larger than the tilting term. So the net result was that the vorticity tendency showed a strong positive value. It can be easily seen that the vorticity tendency in the southeastern quadrant of the mesoscale vortex increased obviously with time, and the vorticity enhancement was the most intensive, which was favorable for the intensification of the upward motion. This probably was the most important reason why the heavy rainfall occurred there. In addition, it can also be seen that the convection term was very important during the development of the mesoscale systems.

In summary, the divergence term and the horizontal advection term related to atmospheric horizontal motions made opposite contributions to the vorticity tendency at a certain pressure level. The divergence term in the lower troposphere was a positive contributor and so was the horizontal advection term in the middle troposphere. The convection term was a positive contributor and the tilting term was a negative contributor in the middle troposphere, but the contributions of these two terms were not always opposite in the lower troposphere. The vorticity tendency was the net result of the various terms of the vorticity equation. The local variability of the vorticity in the southeastern quadrant of the mesoscale vortex was large and the vertical transport of vorticity was strong, which was favorable for the development of

the upward motion and then the enhancement of rainfall. The balance between the divergence term and the horizontal advection term was consistent with the results of Chen and Zhang (2004). The relative vorticity is positive when the wind field is rotating cyclonically. When an air parcel is converging toward the vorticity center, the divergence term $-(\zeta + f)(\frac{\partial u}{\partial x} + \frac{\partial v}{\partial y}) > 0$. Meanwhile, if the air parcel is moving from the low vorticity area toward the high vorticity area, the advection term $-(u\frac{\partial \zeta}{\partial x} + v\frac{\partial \zeta}{\partial y} + v\frac{\partial f}{\partial y}) < 0$. Similarly, considering all the different three-dimensional distributions of vorticity and divergence, such counteracting effects are inevitable.

4.3.2 Local change of vorticity

Vertical profiles of domain-averaged vorticity, (divergence) and vertical velocity over domain A are shown in Fig. 9. The maximum vertical velocity was located around 600 hPa, with a peak value of nearly 0.2 m s^{-1} when the inverted typhoon trough started to develop intensively and the mesoscale vortex formed. At 1000 BT 27 August, the peak value of the convection term appeared around 550 hPa (Fig. 8a) and climbed to 500 hPa by 1400 BT 27 August (Fig. 8b). It can be seen that the peak value of the vertical velocity and that of the vertical transport term were close to each other. The upward transport of relative vorticity from low levels enhanced the local variation of the cyclonic vorticity in the middle troposphere, especially during the developing stage of the inverted typhoon trough and the formative stage of the mesoscale vortex. It can also be noted that convergence (divergence) prevailed below (above) 650 hPa, resulting in the increase (decrease) of the vertical vorticity. Consequently, the divergence term in the lower troposphere made a positive contribution to the vorticity tendency and the divergence term in the middle and upper troposphere made a negative contribution.

Figure 8c shows the domain-averaged vertical profiles of the various vorticity equation terms over domain A when the mesoscale vortex weakened, which was different from Figs. 8b and 8d. There was evident negative vorticity tendency below 350 hPa. The effects of the horizontal advection term and the divergence

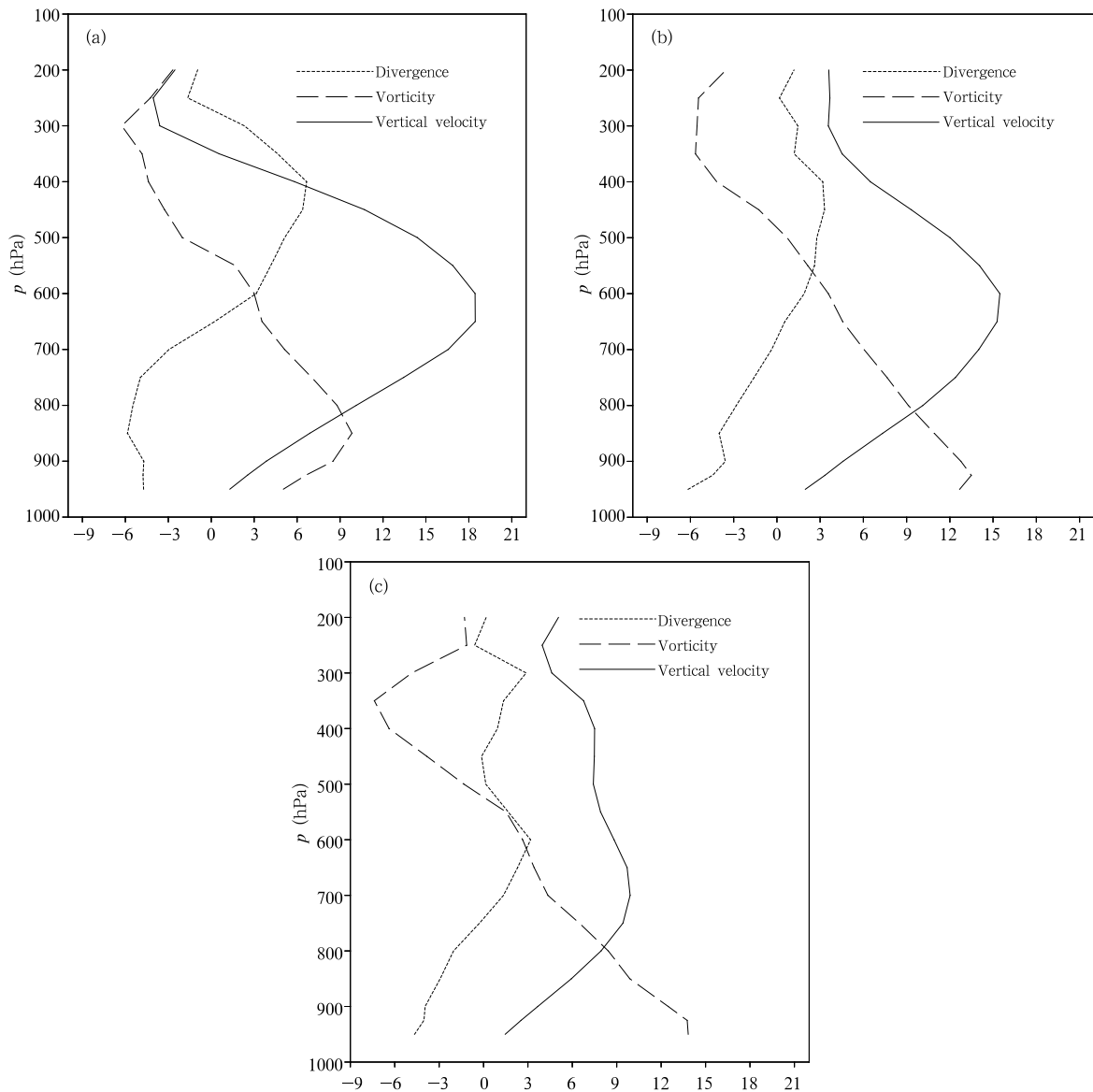


Fig. 9. Vertical profiles of regionally averaged vorticity (10^{-5} s^{-1}), divergence (10^{-5} s^{-1}), and vertical velocity (10^{-2} m s^{-1}) over domain A at 1000 BT (a), 1400 BT (b), and 1800 BT (c) 27 August.

term were weak in the middle and upper troposphere, and especially the horizontal advection term produced a negative contribution between 570 and 400 hPa. A certain balance existed between the vertical transport term and the tilting term. The net result of their counteractions was that negative vorticity tendency, i.e., decreased vorticity with time, occurred and the mesoscale vortex weakened and disappeared. Moreover, the domain-averaged upward motion noticeably weakened (Fig. 9c) at the corresponding time, with

the height of its peak value descending to 700 hPa and the peak value decreased, i.e., the upward transport of positive vorticity decreased from low to upper levels. The height of divergence in the low troposphere dropped to under 780 hPa. The divergence in the upper troposphere also dwindled prominently, with the non-divergence level located between 500 and 450 hPa. In addition, the pumping effect weakened in the upper troposphere, so the effects of the divergence term and the vertical transport term weakened significantly and

then led to a negative local vorticity change.

The above analyses suggest that the increase of low-level positive vorticity was caused by horizontal convergence, while the increase of high-level positive vorticity was related to upward vertical transport of vorticity from low levels. Consequently, on the one hand, the development of the inverted typhoon trough and the formation of the mesoscale vortex were attributed to the production of low-level vorticity; on the other hand, they benefited from the vertical transport of vorticity in the low and middle troposphere.

5. Conclusions

The heavy rainfall event occurred under such an environment that the low-level jet induced by Typhoon Aere and the subtropical high continuously transported water vapor and instability to Shandong Province. It was initially triggered by strong convergence between the strong and weak winds above the inverted typhoon trough. The northward transport of water vapor and momentum in the periphery of the typhoon depression promoted the development of the inverted typhoon trough and the meso- β vortex, and finally the heavy rainfall.

Analyses of the vorticity budget equation suggest that the divergence term in the low troposphere, the horizontal advection term and the vertical transport term in the middle troposphere, were main contributors to positive vorticity. The divergence term and the advection term made opposite contributions to the vorticity tendency. The divergence term in the low troposphere made a positive contribution and the horizontal advection term in the middle troposphere made a negative contribution. The vorticity tendency was the net result of their counteractions. The enhancement of positive vorticity tendency was favorable for the development of the inverted typhoon trough and the mesoscale vortex. Furthermore, the possible reason why the heavy rainfall occurred in the southeast of the vortex was elucidated. The increase of the low-level positive vorticity was caused by horizontal convergence, while the increase of the high-level positive vorticity was related to the upward transport of vorticity from the lower troposphere.

REFERENCES

- Anthes, R. A., 1990: The metamorphosis of Hurricane Hazel revisited. *Extratropical Cyclones: The Erik Palmén Memorial Volume*, C. Newton and E. O. Holopainen, Eds., Amer. Meteor. Soc., 240–249.
- Atallah, E. H., and L. F. Bosart, 2003: The extratropical transition and precipitation distribution of hurricane Floyd (1999). *Mon. Wea. Rev.*, **131**, 1063–1081.
- Bei Naifang, Zhao Sixiong, and Gao Shouting, 2003: A numerical simulation of sudden heavy rainfall occurred in Wuhan and Huangshi during July of 1998. *Chinese J. Atmos. Sci.*, **27**(3), 399–418. (in Chinese)
- Bosart, L. F., and F. H. Carr, 1978: A case study of excessive rainfall centered around Wellsville, New York, 20–21 June 1972. *Mon. Wea. Rev.*, **106**, 348–362.
- Chen Min and Zhang Yongguang, 2004: Vorticity budget investigation of a simulated long-lived mesoscale vortex in South China. *Adv. Atmos. Sci.*, **21**(6), 928–940.
- DiMego, G. J., and L. F. Bosart, 1982a: The transformation of tropical storm Agnes into an extratropical cyclone. Part I: The observed fields and vertical motion computations. *Mon. Wea. Rev.*, **110**, 385–411.
- DiMego, G. J., and L. F. Bosart, 1982b: The transformation of tropical storm Agnes into an extratropical cyclone. Part II: Moisture, vorticity, and kinetic energy budgets. *Mon. Wea. Rev.*, **110**, 412–433.
- Ding Zhiying and Chen Jiukang, 1995: Diagnosis, comparative analysis and simulation of typhoons with different rainfall intensities. *Journal of Nanjing Institute of Meteorology*, **18**(2), 234–241.
- Ding Zhiying, Zhang Xingqiang, He Jinhai, et al., 2001: The study of storm rainfall caused by interaction between the non-zonal high level jet streak and the far distant typhoon. *Chinese J. Tropical Meteor.*, **17**(2), 144–154. (in Chinese)
- Feng Wuhu, Cheng Linsheng, and Cheng Minghu, 2000: Nonhydrostatic numerical simulation for the “96.8” extraordinary heavy rainfall and the developing structure of mesoscale system. *Acta Meteor. Sinica*, **59**(3), 294–307. (in Chinese)
- Jiang Jixi and Xiang Xukang, 1997: A primary study of the extreme rainfall event in early August 1996 over Hebei Province. *Meteorology Monthly*, **23**(7), 19–23. (in Chinese)

- Jiang Shangcheng, Zhang Tan, Zhou Mingsheng, et al., 1981: The hard rainstorms in North China induced by a landed northward moving and decaying typhoon-hard rainstorms of semi-tropical systems. *Acta Meteor. Sinica*, **39**(1), 18–27. (in Chinese)
- Jiang Shangcheng, 1983: A synoptic model of the hard rainstorm in westly belt affected by the far distant typhoon. *Acta Meteor. Sinica*, **41**(2), 147–158. (in Chinese)
- Jiang Yongqiang, Wang Changyu, Zhang Weihuan, et al., 2003: Numerical simulation of extremely heavy rain and mesoscale low vortex in an inverted typhoon trough. *Acta Meteor. Sinica*, **61**(3), 312–322. (in Chinese)
- Li Ying, Chen Lianshou, and Xu Xiangde, 2005: Numerical experiments of the impact of moisture transportation on sustaining of the landfalling tropical cyclone and precipitation. *Chinese J. Atmos. Sci.*, **29**(1), 91–98. (in Chinese)
- Palmén, E., 1958: Vertical circulation and release of kinetic energy during the development of Hurricane Hazel into an extratropical cyclone. *Tellus*, **10**, 1–23.
- Sheng Chunyan, Xue Deqiang, Lei Ting, et al., 2006: Comparative experiments between effects of Doppler radar data assimilation and increasing horizontal resolution on short-range prediction. *Acta Meteor. Sinica*, **64**(3), 293–307. (in Chinese)
- Sun Jianhua and Zhao Sixiong, 2000: Diagnoses and simulations of typhoon (Tim) landing and producing heavy rainfall in China. *Chinese J. Atmos. Sci.*, **24**(2), 223–237. (in Chinese)
- Sun Jianhua, Qi Linlin, and Zhao Sixiong, 2006: A study on mesoscale convective systems of the severe heavy rainfall in North China by “9608” typhoon. *Acta Meteor. Sinica*, **64**(1), 57–71. (in Chinese)
- Yang Shuai and Gao Shouting, 2007: Three-dimensional divergence equation and its diagnosis to storm rainfall system. *Chinese J. Atmos. Sci.*, **31**(1), 167–179. (in Chinese)
- Yang Shuai, Gao Shouting, and Wang Donghai, 2007: A study of Richardson number and instability in moist saturated flow. *Chinese J. Geophys.*, **50**(2), 377–386. (in Chinese)
- Ye Chengzhi, Pan Zhixiang, Cheng Rui, et al., 2007: The numerical research of the primary mechanism of the offing reinforcement of Typhoon Rananim based on AREM. *Acta Meteor. Sinica*, **65**(2), 208–220. (in Chinese)
- Zhao Yu, Gong Dianli, Liu Shijun, et al., 2006: Numerical simulation of forming mechanism for the torrential rain in Shandong Province in August 1999. *Plateau Meteorology*, **25**(1), 95–104. (in Chinese)
- Zhu Hongyan, Chen Lianshou, and Xu Xiangde, 2000: A numerical study of the interactions between typhoon and mid-latitude circulation and its rainfall characteristics. *Chinese J. Atmos. Sci.*, **24**(5), 669–675. (in Chinese)
- Zhu Peijun, Chen Min, Tao Zhuyun, et al., 2002a: Numerical simulation of Typhoon Winnie (1997) after landfall. Part I: Model verification and model clouds. *Acta Meteor. Sinica*, **60**(5), 553–559. (in Chinese)
- Zhu Peijun, Chen Min, Tao Zhuyun, et al., 2002b: Numerical simulation of Typhoon Winnie (1997) after landfall. Part II: Structure evolution analysis. *Acta Meteor. Sinica*, **60**(5), 560–567. (in Chinese)